

A. Poszwa

Two-Electron Spherical Quantum Dot in a Magnetic Field

Received: 16 May 2016 / Accepted: 12 July 2016 / Published online: 18 July 2016
© The Author(s) 2016. This article is published with open access at Springerlink.com

Abstract We investigate three-dimensional, two-electron quantum dots in an external magnetic field B . Due to mixed spherical and cylindrical symmetry the Schrödinger equation is not completely separable. Highly accurate numerical solutions, for a wide range of B , have been obtained by the expansion of wavefunctions in double-power series and by imposing on the radial functions appropriate boundary conditions. The asymptotic limit of a very strong magnetic field and the 2D approach have been considered. Ground state properties of the two-electron semiconductor quantum dots are investigated using both the 3D and 2D models. Theoretical calculations have been compared with recent experimental results.

1 Introduction

The influence of spatial confinement on properties of quantum systems have been widely studied in the literature and remains subject of continuous interest in both theoretical and experimental fields [1–5]. One of the most interesting confined quantum systems is the two-electron *Hooke's-law atom* (HA) also known as *hookium* or *harmonium* [6]. The HA refers to a model system composed of two electrons interacting by the Coulombic potential and confined in an external harmonic potential. Many applications for this system ensues from some unique properties of the HA. For the parabolic confinement the two-electron Hamiltonian separates. This property significantly simplifies the two-particle Schrödinger equation leading, in fact, to the one-dimensional radial problem. We note that the separability of the Schrödinger equation describing many interacting particles is rather exceptional. In particular, it is possible when interactions between disjoint pairs of particles, interacting by arbitrary two-particle potentials, are harmonic [7,8]. For the HA the Schrödinger equation not only separates exactly but also, for a set of the coupling constants, closed-form analytical solutions exist [9,10]. This is of particular importance for the understanding of the role of electron–electron interaction and correlation effects.

When the electron mass is replaced by the relevant effective mass and the e–e interaction coupling constant is supplemented by the dielectric constant of semiconductor, the HA atom may be regarded to as a two-electron quantum dot (QD). During last few decades many theoretical and experimental studies on QDs have been performed within parabolic confinement models as well as beyond this approximation. Both the 2D and 3D QD's have been investigated in a framework of strict quantum-mechanical and semiclassical approaches, including also effects of an external magnetic field [11–30]. Semiclassical solutions for a two-electron QD in a magnetic field have been investigated in terms of action-angle variables using the classical adiabatic approximation [19]. Spin-singlet and spin-triplet transitions have been studied and the magnetic moment and susceptibility have been obtained as functions of the magnetic field [20].

A. Poszwa (✉)
Department of Physics and Computer Methods, University of Warmia and Mazury in Olsztyn, ul. Słoneczna 54, 10-710 Olsztyn,
Poland
E-mail: poszwa@matman.uwm.edu.pl

Particular analytical solutions for two electrons in a 3D harmonic potential and in a magnetic field have been obtained for a set of confinement frequencies, using parabolic and cylindrical coordinates [26]. Using some of these solutions, exact density functionals for two electron systems in an external magnetic field have been constructed in a frame of the density functional theory (DFT) and the current DFT (CDFT) [27]. Furthermore, the energy eigenvalues, electron densities, paramagnetic current densities, pair densities and Kohn–Sham orbitals for the HA in B field have been calculated numerically. However, as has been pointed out in [27], extended precision arithmetic is required to improve the computed results.

The aim of this paper is to perform numerical high-precision calculations for a Hooke's atom in an axial magnetic field, for a wide range of the magnetic field intensity. The problem is studied using the power-series expansion method. This method was first formulated by Kravchenko et al. and applied to the hydrogen atom in a magnetic field [31–34]. The method bases on using boundary conditions determined by the asymptotic behavior of solutions at large distances. The asymptotic limit of a very strong magnetic field, when the system may be described by an effective one-dimensional potential, has been considered. In this context, the problem of a continuous reduction of spatial dimensions is examined.

Finally, we investigate ground-state magnetic properties of the two-electron semiconductor QD's, using parameters characteristic for GaAs. In particular, we study the B -field evolution of the chemical potential and the addition energy, taking into account experimentally determined values for the confinement frequencies [21]. The 3D and the 2D models are considered.

2 Formulation of the Problem

The Schrödinger Hamiltonian describing two electrons with masses m_e interacting by a Coulomb potential, confined in a harmonic potential and subject into an external magnetic field, described by the vector $\mathbf{A}(\mathbf{r}) = \frac{1}{2} \mathbf{B} \times \mathbf{r}$, where $\mathbf{B} = (0, 0, B)$, in Gauss units reads

$$H_{\text{tot}} = \sum_{i=1}^2 \left[\frac{1}{2m_e} \left(\mathbf{p}_i + \frac{e}{c} \mathbf{A}(\mathbf{r}_i) \right)^2 + \frac{1}{2} m_e \omega_0^2 r_i^2 \right] + \frac{e^2}{|\mathbf{r}_1 - \mathbf{r}_2|} + H_{\text{spin}}, \quad (1)$$

where

$$H_{\text{spin}} = g\mu_B (\mathbf{s}_1 + \mathbf{s}_2) \cdot \mathbf{B} = g\mu_B B \hat{S}_z. \quad (2)$$

Here $\mu_B = \hbar e / (2m_e c)$ is the Bohr magneton, S_z is the projection of the total spin and $g = -2$. The triplet spin states of two electrons in the magnetic field split into three distinct levels, while the singlet states remain unchanged. For triplets, we shall consider only the lowest components corresponding to $S_z = 1$. Thus, the spin contribution to the Zeeman shift for a spin-singlet and for a spin-triplet state may be respectively written as

$$E_{\text{spin}} = g\mu_B B S_z, \quad (3)$$

where $S_z = 0, 1$.

Upon the substitution

$$\mathbf{R} = \{X, Y, Z\} = \frac{1}{2}(\mathbf{r}_1 + \mathbf{r}_2), \quad \mathbf{r} = \{x, y, z\} = \mathbf{r}_1 - \mathbf{r}_2 \quad (4)$$

the spatial part of the Hamiltonian (1) separates to two *one-particle* parts: the center-of-mass Hamiltonian

$$H_{\text{c.m.}} = -\frac{\hbar^2}{2M} \Delta_{\mathbf{R}} + \frac{1}{2} M [\omega_\rho^2 (X^2 + Y^2) + \omega_0^2 Z^2] + \frac{1}{2} \omega_c \hat{L}_z, \quad (5)$$

where $M = 2m_e$, $\omega_\rho = \sqrt{\omega_0^2 + \omega_c^2/4}$, $\omega_c = eB/(m_e c)$ and the Hamiltonian describing the relative motion

$$H = -\frac{\hbar^2}{2\mu} \Delta + \frac{1}{2} \mu [\omega_\rho^2 (x^2 + y^2) + \omega_0^2 z^2] + \frac{1}{r} + \frac{1}{2} \omega_c \hat{l}_z, \quad (6)$$

where $\mu = m_e/2$. The angular momentum operators \hat{L}_z and \hat{l}_z are defined in the standard way. Consequently, the total energy of the system is given by

$$E_{\text{tot}} = E_{\text{c.m.}} + E + E_{\text{spin}}. \quad (7)$$

For further calculations, it is convenient to introduce the following scaling

$$\mathbf{R} := \mathbf{R} \sqrt{\frac{\mu \omega_\rho}{\hbar}}, \quad \mathbf{r} := \mathbf{r} \sqrt{\frac{\mu \omega_\rho}{\hbar}} \quad (8)$$

transforming the Schrödinger equation of the c. m. and the relative motion, respectively to the forms

$$\left(-\frac{1}{2} \Delta_{\mathbf{R}} + 8[X^2 + Y^2] + 8a^2 Z^2 \right) \Psi_{\text{c.m.}} = \frac{4E_{\text{c.m.}} - 2\gamma M_z}{\Omega} \Psi_{\text{c.m.}}, \quad (9)$$

where $a = \omega_0/\omega_\rho$ is the anisotropy parameter, M_z is the magnetic quantum number of the c. m. motion and

$$\left(-\frac{1}{2} \Delta + \frac{1}{2} r^2 [a^2 + (1-a^2) \sin^2 \vartheta] + \frac{s}{2r} \right) \Psi = \mathcal{E} \Psi. \quad (10)$$

We have introduced above the eigenvalue \mathcal{E} and following parameters

$$s = \sqrt{\frac{2}{\Omega}}, \quad \Omega = \sqrt{\Omega_0^2 + \frac{1}{4} \gamma^2}, \quad \Omega_0 = \frac{\omega_0}{\omega_h}, \quad (11)$$

where $\hbar \omega_h = E_h$ and $\gamma = B/B_0$. The atomic unit of energy and magnetic field respectively are one hartree $E_h = m_e e^4 / \hbar^2$ and $B_0 = m_e^2 e^3 c / \hbar^3$. The anisotropy parameter may be expressed also using dimensionless frequencies, as $a = \Omega_0 / \Omega$.

The solution to the c.m. part is well known. In particular, energies (in hartrees) read

$$E_{\text{c.m.}} = (2N_0 + |M_z| + 1)\Omega + \left(N_z + \frac{1}{2} \right) \Omega_0 + \frac{1}{2} \gamma M_z, \quad (12)$$

where $N_0, N_z = 0, 1, \dots$. In further calculations we shall refer to the c.m. energy as to the ground state energy $E_{\text{c.m.}} = \Omega + \Omega_0/2$. The sum of the first and the third terms in (12) gives the Fock–Darwin levels [35,36]. We note that, due to the presence of the confinement, the infinite degeneracy of Landau levels corresponding to $M_z < 0$, is removed. As a consequence, contrary to the Landau orbits, centers of the Fock–Darwin orbits are localized on the z -axis, for every M_z .

Energies (in hartrees) of the relative motion are given by

$$E = \mathcal{E} \Omega + \frac{1}{2} \gamma m, \quad (13)$$

where \mathcal{E} is the eigenvalue of the Eq. (10) and m is the magnetic quantum number of the relative motion. One should be pointed out that for nonzero B , we have $a < 1$ and the potential depends on ϑ . This causes the main difficulties in the problem. The Schrödinger equation (10) does not separate.

3 Power-Series Solutions

Using spherical coordinates, the relative motion wavefunction may be expressed in the form of a double power series in r and the sine of ϑ [31]. Thus, solutions to the Eq. (10) may be supposed in the form

$$\Psi(r, \vartheta, \phi) = e^{im\phi} (r \sin \vartheta)^{|m|} (r \cos \vartheta)^\nu e^{-\frac{1}{2} r^2 [a + (1-a) \sin^2 \vartheta]} \psi(r, \vartheta), \quad (14)$$

where $\nu = 0$ or 1 is the z -parity quantum number and

$$\psi(r, \vartheta) = \sum_{k=0}^{\infty} (r \sin \vartheta)^{2k} g_{2k}(r). \quad (15)$$

After substituting Ψ into Eq. (10) we obtain for radial functions $g_{2k}(r)$ the system of second-order coupled equations

$$\begin{aligned} g''_{2k} + 2 \left(\frac{2k + |m| + \nu + 1}{r} - ra \right) g'_{2k} + \left(2\mathcal{E}_a - 4k - \frac{s}{r} \right) g_{2k} \\ - \frac{2(1-a)}{r} g'_{2k-2} + 4(k+1)(k+|m|+1) g_{2k+2} = 0, \end{aligned} \quad (16)$$

where $\mathcal{E}_a = \mathcal{E} - |m| - a(v + 1/2) - 1$. In order to determine energies and wavefunctions, we expand every radial function into power series

$$g_{2k}(r) = \sum_{i=0}^{\infty} A_{i,2k} r^i. \quad (17)$$

After substituting the above expansions to Eq. (16) we obtain for the coefficients recurrence relation

$$\begin{aligned} & i(i+1+2(2k+|m|+v))A_{i,2k} - 2i(1-a)A_{i,2k-2} - sA_{i-1,2k} \\ & + 2(\mathcal{E}_a - 2k + a(2-i))A_{i-2,2k} \\ & + 4(k+1)(k+|m|+1)A_{i-2,2k+2} = 0. \end{aligned} \quad (18)$$

Supposing $A_{i<0,2k} \equiv 0$ and $A_{i,2k<0} \equiv 0$, one follows from the last relation that all $A_{0,2k}$, for $k = 0, 1, \dots$, can be chosen as arbitrary and the remaining coefficients may be calculated from Eq. (18), by starting from these initial coefficients. Defining a particular solution $\psi^{(p)}$ by setting $A_{0,2k}^{(p)} = \delta_{kp}$ and $A_{i,2k}^{(p)} \equiv 0$, for $k > q$, where q is some cut-of parameter (an angular cut-of), we can calculate the other coefficients $A_{i,2k}^{(p)}$ from Eq. (18), until $i = I$. Here, I is the radial cut-of. In this manner we can generate a set of approximate particular solutions for $p = 0, 1, \dots, q$,

$$\psi^{(p)}(r, \vartheta) = \sum_{k=0}^q (r \sin \vartheta)^{2k} \sum_{i=0}^I A_{i,2k}^{(p)} r^i. \quad (19)$$

Then, a general solution ψ is expressed as a linear combination of $\psi^{(p)}$,

$$\psi = \sum_{p=0}^q C_p \psi^{(p)}. \quad (20)$$

Thus, the approximate radial amplitudes for $k = 0, 1, \dots, q$ read

$$g_{2k}(r) = \sum_{p=0}^q C_p \sum_{i=0}^I A_{i,2k}^{(p)} r^i. \quad (21)$$

The linear parameters C_p and energy E are determined by imposing on functions g_{2k} asymptotic boundary conditions, that ensure square-integrability of the total wavefunction.

By looking for asymptotic solutions to the Eq. (16) we can find that asymptotically these equations are satisfied by functions

$$\lim_{r \rightarrow \infty} g_{2k}(r) = \text{const}(k) \times r^{\alpha-2k}, \quad (22)$$

where $\alpha = \mathcal{E}_a/a$. The functions given above determine the leading approximations to the exact radial functions at large r . The boundary conditions determined by the functions (22) read

$$\eta_k = \lim_{r \rightarrow \infty} \frac{g'_{2k}(r)}{g_{2k}(r)} = \frac{\alpha - 2k}{r}, \quad (23)$$

where $k = 0, 1, \dots, q$. These simple boundary conditions are sufficient for calculation of energy levels for the HA in the magnetic field. By matching logarithmic derivatives of functions (21) with those ones given by the Eq. (23), at a finite joining radius $r = R$, we obtain a linear system

$$\sum_{p=0}^q D_{kp} C_p = 0, \quad k = 0, \dots, q, \quad (24)$$

where

$$D_{kp} = \sum_{i=0}^I (i - \eta_k) A_{i,2k}^{(p)} R^i. \quad (25)$$

Energies are determined from the condition of the linear dependence of the system (24) which leads to the nonlinear equation for energy levels,

$$\det D(E) = 0. \quad (26)$$

The accuracy of energies in a given (R, I, q) -approximation is determined by stability of results, for increasing parameters R, I and q .

3.1 The Limit of Strong B Field

In the classical treatment of this system, the dynamics in the limit of strong magnetic field, can be effectively separated due to different time scales connected with the lateral and the vertical motion. This allows for application of a classical adiabatic approximation. In the lowest order of this approximation, the classical Hamiltonian function is averaged over the *fastest* angle of the unperturbed motion, after transforming coordinates to action-angle variables [19]. A natural extension of this method to the quantum system is averaging the Hamiltonian operator over the Fock–Darwin orbitals.

Therefore, using this approximation, the part of the Schrödinger equation including the effective coulombic interaction, can be written as

$$\left[-\frac{d^2}{dz^2} + U_{\text{eff}}(z) \right] \psi(z) = E_z^{\text{eff}} \psi(z), \quad (27)$$

where

$$U_{\text{eff}}(z) = \left(\frac{\Omega_0}{2} \right)^2 z^2 + \left\langle \frac{1}{r} \right\rangle. \quad (28)$$

Energies of the 3D system, in this effective 1D-approximation, are given by

$$E^{\approx 1D} = (2n + |m| + 1)\Omega + \frac{1}{2}\gamma m + E_z^{\text{eff}}, \quad (29)$$

where the sum of the first two terms describes energies of the lateral motion of noninteracting particles. The effective Coulomb repulsion potential reads

$$\left\langle \frac{1}{r} \right\rangle = \left\langle nm \left| \frac{1}{\sqrt{\rho^2 + z^2}} \right| nm \right\rangle, \quad (30)$$

where averaging is performed over normalized eigenstates of the Hamiltonian $H^{2D}(\rho) = -\Delta + \Omega^2 \rho^2/4$, given by

$$\psi_{nm}(\rho, \phi) = N_1 \frac{e^{im\phi}}{\sqrt{2\pi}} \rho^{|m|+1/2} e^{-\Omega \rho^2/4} F\left(-n, 1 + |m|, \frac{\Omega}{2} \rho^2\right), \quad (31)$$

where

$$N_1 = \frac{\Omega^{(|m|+1)/2}}{|m|!} \sqrt{\frac{\Gamma(1+n+|m|)}{2^{|m|}n!}}. \quad (32)$$

By averaging over the ground state we get

$$\left\langle \frac{1}{r} \right\rangle = \sqrt{\frac{\pi\Omega}{2}} e^{\Omega z^2/2} \text{erfc}\left(\sqrt{\frac{\Omega}{2}}|z|\right), \quad (33)$$

where

$$\text{erfc}(x) = \frac{2}{\sqrt{\pi}} \int_x^\infty e^{-t^2} dt \quad (34)$$

is the complementary error function [37]. Finally,

$$U_{\text{eff}}(z) = \left(\frac{\Omega_0}{2} \right)^2 z^2 + \sqrt{\frac{\pi\Omega}{2}} e^{\Omega z^2/2} \text{erfc}\left(\sqrt{\frac{\Omega}{2}}|z|\right). \quad (35)$$

We note that since $\text{erfc}(0) = 1$, the effective potential (28) is finite at $z = 0$, where it takes the value

$$U_{\text{eff}}(0) = \sqrt{\frac{\pi\Omega}{2}}. \quad (36)$$

The potential has been plotted in Fig. 1.

Using the asymptotic expansion of the complementary error function [37] one obtains

$$\lim_{|z| \rightarrow \infty} \left\langle \frac{1}{r} \right\rangle = \frac{1}{|z|} \left(1 - \frac{1}{\Omega z^2} + \frac{3}{(\Omega z^2)^2} - \frac{15}{(\Omega z^2)^3} + \dots \right). \quad (37)$$

We can see that for increasing Ω , the first term in the asymptotic expansion dominates. Thus, in the limit $\Omega \rightarrow \infty$, the effective potential $U_{\text{eff}}(z)$ approaches the function

$$U(z) = 1/|z| + (\Omega_0 z/2)^2, \quad (38)$$

for all z . The result is rather natural and intuitively understandable. For strong B , the motion of electrons is constrained to almost one-dimensional region along the magnetic field direction. Since the available space for two electrons becomes smaller they avoid each other more effectively and their average distance increases. This means that $r \approx z$ and for the e–e interaction potential we can use the approximation $1/r \approx 1/|z|$. As a consequence, the Schrödinger Hamiltonian separates, in the cylindrical coordinates. The separation of the dynamics obtained here confirms the limit of $B \rightarrow \infty$ discussed in a frame of the effective charge method [23].

We can note that the result obtained in this section is important from a point of view of the Wigner crystallization. Due to presence of the lateral confinement, centers of the Landau orbits are localized on the z -axis. For increasing B , the orbits become smaller. On the other hand the vertical confinement produces a local minimum in the effective interacting potential. Therefore, a necessary condition for an occurrence of the Wigner crystallization is fulfilled.

3.2 Semiconductor QD's

In this section we apply the model to study ground-state electronic properties of the two-electron QD's in a magnetic field. Introducing into the Hamiltonian (1) material parameters typical for GaAs: the electron effective mass $m^* = 0.067m_e$, the dielectric constant $\epsilon = 12$ and the effective Landé factor $g^* = -0.44$, leads to the same forms of Eqs. (10), (12) and (13) with s, Ω replaced respectively by

$$s_\kappa = \frac{1}{\epsilon} \sqrt{\frac{2\kappa}{\Omega_\kappa}}, \quad \Omega_\kappa = \sqrt{\Omega_0^2 + \frac{1}{4}\kappa^{-2}\gamma^2}, \quad (39)$$

where $\kappa = m^*/m_e$. We investigate the ground-state energy, the chemical potential and the addition energy of a QD as functions of the magnetic field. The B -field evolution of these quantities can be directly studied by single electron capacitance spectroscopy or by tunneling spectroscopy [14,21]. The chemical potential is given by

$$\mu(N, B) = E_{\text{tot}}(N, B) - E_{\text{tot}}(N-1, B), \quad (40)$$

where $E_{\text{tot}}(N, B)$ is the total ground-state energy of the QD with N electrons. For $N = 2$ one obtains

$$\mu(2, B) = \mathcal{E}_\kappa \Omega_\kappa + \frac{1}{2}\gamma m \kappa^{-1} + \frac{1}{2}\gamma g^* \left(S_g - \frac{1}{2} \right), \quad (41)$$

where \mathcal{E}_κ denotes eigenvalue of the Eq. (10) with $s = s_\kappa$. Here S_g is the total spin of the QD corresponding to the ground state. The most direct probe of the electron–electron interaction and correlation effects in the QD is the difference $\Delta\mu = \mu(2, B) - \mu(1, B)$, named also the addition energy [19,22]. The addition energy takes the form

$$\Delta\mu = (\mathcal{E}_\kappa - 1)\Omega_\kappa + \frac{1}{2}\gamma m \kappa^{-1} + \frac{1}{2}\gamma g^* \left(S_g - \frac{1}{2} \right) - \frac{1}{2}\Omega_0. \quad (42)$$

Energies of the 2D QD in the magnetic field have been obtained by generalization of the power series expansion method, used for the 2D hydrogen atom [34].

4 Results

According to the Pauli exclusion principle the total wavefunction of the system changes sign upon the exchange of two electrons. This leads to the relationship between the total spin and orbital quantum numbers. Writing the total wavefunction of two electrons as $\Psi(1, 2) = \Psi_{c.m.}(\mathbf{R})\psi(\mathbf{r})\chi(1, 2)$ we can easily find that the operation of exchanging two electrons leads to $\Psi(2, 1) = \Psi_{c.m.}(\mathbf{R})\psi(-\mathbf{r})\chi(2, 1)$. Taking into account that the singlet (triplet) spin state is antisymmetric (symmetric) with respect to interchanging of the electrons we have $\chi(2, 1) = (-1)^{S+1}\chi(1, 2)$. Therefore, the total spin of two electrons for the spherically-symmetric system and for the 3D axially-symmetric system is determined by the condition $(-1)^S = (-1)^l$ and $(-1)^S = (-1)^{|m|+v}$, respectively. It is worth to point out that for the 2D system with the circular symmetry the total spin of two electrons is determined only by the magnetic quantum number, according to the relation $(-1)^S = (-1)^{|m|}$. Thus, the singlet (triplet) spin states correspond to even (odd) m . However, this is not true for the 3D cylindrically-symmetric system because of the z -parity contribution to the symmetry of the relative motion wavefunction.

In Tables 1 and 2 are given total energies of the lowest three spin-singlet and spin-triplet states, respectively, as functions of the magnetic field, for confinement frequencies $\Omega_0 = 0.1$ and 0.5 . The maximal absolute error of each values does not exceed ± 1 in the last digit, in all of the tables. The comprehensive analysis of the convergence of the method may be found in [31, 32]. The lowest energies are compared with the previous most accurate results by Zhu and Trickey [27]. The agreement between the results is excellent. One can see that for $B = 0$, the ground state is a singlet. The singlet state remains as the ground state only for low magnetic fields. As the magnetic field increases this state rises in energy while the triplet state drops and for certain value of γ we can observe the singlet–triplet (ST) transition, in the ground state. For confinement frequencies $\Omega_0 = 0.1$ and $\Omega_0 = 0.5$, the first ST transitions occur at $\gamma \approx 0.036$ and at $\gamma \approx 0.27$, respectively.

Table 3 presents the relative motion energies E^{3D} , energies obtained within the effective 1D-approximation $E^{\approx 1D} = \Omega + E_z^{\text{eff}}$ and energies $E^{1D} = \Omega + E_z$, where E_z correspond to the potential $U(z)$. In the last three columns Coulombic energies (CE) are displayed. The CE are defined as differences between the relative motion

Table 1 Total energies in hartrees for the HA in B fields for three lowest singlet states $(m, v) = (0, 0)$

Ω_0	γ	E_{tot}	E_{tot}	E_{tot}
0.1	0	1/2	0.627658039887	4/5
	0.01	0.500347496740	0.682994780073	0.870079923939
	0.1	0.500347 ^a	0.730803354433	0.868950357224
		0.532171302211		
	0.34641	0.532171 ^a	0.878633268647	1.03689825583
		0.745667680755		
	1	0.745668 ^a	1.55174332573	1.70950414580
		1.39721803775		
	5	1.397218 ^a	5.57294069223	5.74914163530
		5.39824994221		
	10	5.398251 ^a	10.5763165067	10.7565656431
		10.3986512404		
	20	10.39865 ^a	20.57829864	20.76084636
	0	20.39896252		
0.5	0	2	2.79361389787	3.72666383764
	0.1	2.00590387326	2.94924380802	3.91298429342
	1	2.005904 ^a	3.27809645956	4.22241720588
		2.47752326975		
	5	2.477523 ^a	7.12484310081	8.00848396348
		6.36394967542		
	10	6.363950 ^a	12.1641657806	13.0287972693
		11.3874260575		
	20	11.387426 ^a	22.2191449248	23.0789308722
		21.4125949008		
	50	51.4378477967	52.2829179540	53.1555799537
		51.43792 ^a		
	80	81.4472157506	82.3078112835	83.1904860566
	100	101.450970027	102.317850697	103.205290511
	200	101.4549 ^a	202.3429096	203.2438414
		201.4603628		
	400	401.4671	402.3608	403.2725

^a Quoted from Ref. [27]

Table 2 Total energies in hartrees for the HA in B fields for three lowest triplet states $(m, \nu) = (-1, 0)$

Ω_0	γ	E_{tot}	E_{tot}	E_{tot}
0.1	0	0.553172793895	0.711412203792	0.891448313132
	0.01	0.538630379091	0.727602750352	0.919232064434
		0.538630 ^a		
	0.1	0.446038406584	0.603175951229	0.867200725063
		0.446038 ^a		
	0.34641	0.380384757729	0.522801966674	0.698810905997
		0.380385 ^a		
	1	0.382221841307	0.518702445556	0.680684010151
		0.382222 ^a		
	5	0.394748528711	0.561438496167	0.701598063244
0.5		0.394749 ^a		
	10	0.396743424419	0.570154892843	0.744307028010
		0.39674 ^a		
	20	0.397884541	0.574881258	0.754022702
	0	2.35965705992	3.25384094137	4.20662233385
	0.1	2.21788482338	3.19083462043	4.17250302217
		2.217885 ^a		
	1	1.53482727688	2.89744884348	4.27637477277
		1.534827 ^a		
	5	1.27758756480	2.06021561816	2.98060107913
		1.277588 ^a		
	10	1.30766761638	2.06512930763	2.95908827839
		1.307668 ^a		
	20	1.35312870554	2.11670715446	2.98590017916
	50	1.40248195130	2.20462147480	3.06185040809
		1.40250 ^a		
	80	1.42048252837	2.24460211666	3.10640662574
	100	1.42752771141	2.26126375267	3.12693039174
		1.4303 ^a		
	200	1.444549681	2.303369514	3.183998574
	400	1.456196	2.333104	3.228519

^a Quoted from Ref. [27]**Table 3** Dependence on the magnetic field γ (in a. u.) of relative motion energies E^{3D} (3D model), $E^{\approx 1D}$ (effective 1D model) and E^{1D} (1D model)

γ	E^{3D}	$E^{\approx 1D}$	E^{1D}	E_C^{3D}	$E_C^{\approx 1D}$	E_C^{1D}
10	6.11248824694	6.24379269	6.27493781	0.83755044	0.96885488	1
20	11.1501027035	11.2441510	11.2624922	0.88761051	0.98165880	
50	26.1828482966	26.2462845	26.2549995	0.92784880	0.99128499	
80	41.1940908727	41.2472575	41.2531249	0.94096599	0.99413264	
100	51.1984700895	51.2476500	51.2524999	0.94597015	0.99515002	
200	101.2091128	101.248589	101.251250	0.9578628	0.99733906	
300	151.2137567	151.248970	151.250833	0.9629233	0.99813664	
400	201.2165	201.249181	201.250625	0.96585	0.99855564	
500	251.2184	251.249316	251.250500	0.96791	0.99881574	
1000	501.2219	501.249614	501.250250	0.97168	0.99936389	

In the last three columns Coulombic energies are displayed. Energies are given in hartrees. $\Omega_0 = 0.5$

energies of interacting and noninteracting electrons. Let $E^{\text{ind}} = \Omega + (n_z + 1/2)\Omega_0$ denotes the relative motion energy of noninteracting (independent) electrons, for the state $(m = 0, \nu = 0)$. The CE read respectively as $E_C^{3D} = E^{3D} - E^{\text{ind}} = (\mathcal{E} - 1)\Omega - (n_z + 1/2)\Omega_0$, $E_C^{\approx 1D} = E^{\approx 1D} - E^{\text{ind}} = E_z^{\text{eff}} - (n_z + 1/2)\Omega_0$ and $E_C^{1D} = E^{1D} - E^{\text{ind}} = E_z - (n_z + 1/2)\Omega_0$. For $\Omega_0 = 1/2$ we obtain energies $E_z = 5/4, 2.1901169, \dots$. Focusing attention on the lowest state $E_z = 5/4$ ($n_z = 0$) one obtains, $E_C^{1D} = 1$. We can see that, with increasing γ , the relative motion energies and the Coulombic energies of the 3D model evolve monotonically and approach energies of the 1D model.

In Fig. 2 are compared the B -field dependence of the ground-state energy, the chemical potential $\mu(2, B)$ and the addition energy $\Delta\mu = \mu(2, B) - \mu(1, B)$ for the 3D and the 2D QD's with the confinement frequency $\hbar\omega_0 = 2 \text{ meV}$. Energies and a magnetic field intensity are given in 1 meV and 1 T, respectively. The dimensionless

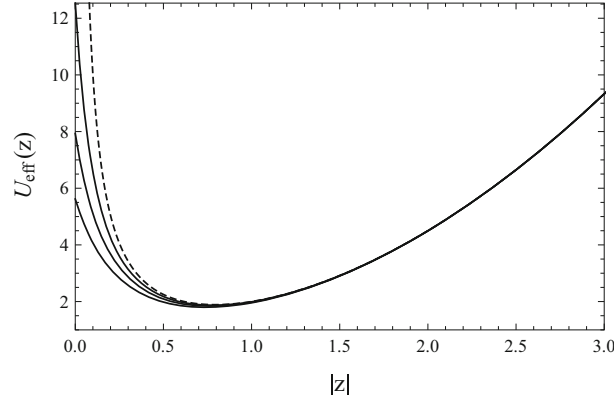


Fig. 1 Effective 1D potential $U_{\text{eff}}(z)$ for $\gamma = 40, 80, 200$ (from below) and comparison with the potential $U(z) = 1/|z| + (\Omega_0 z/2)^2$, corresponding to $\gamma \rightarrow \infty$ (black, dashed). $\Omega_0 = 2$

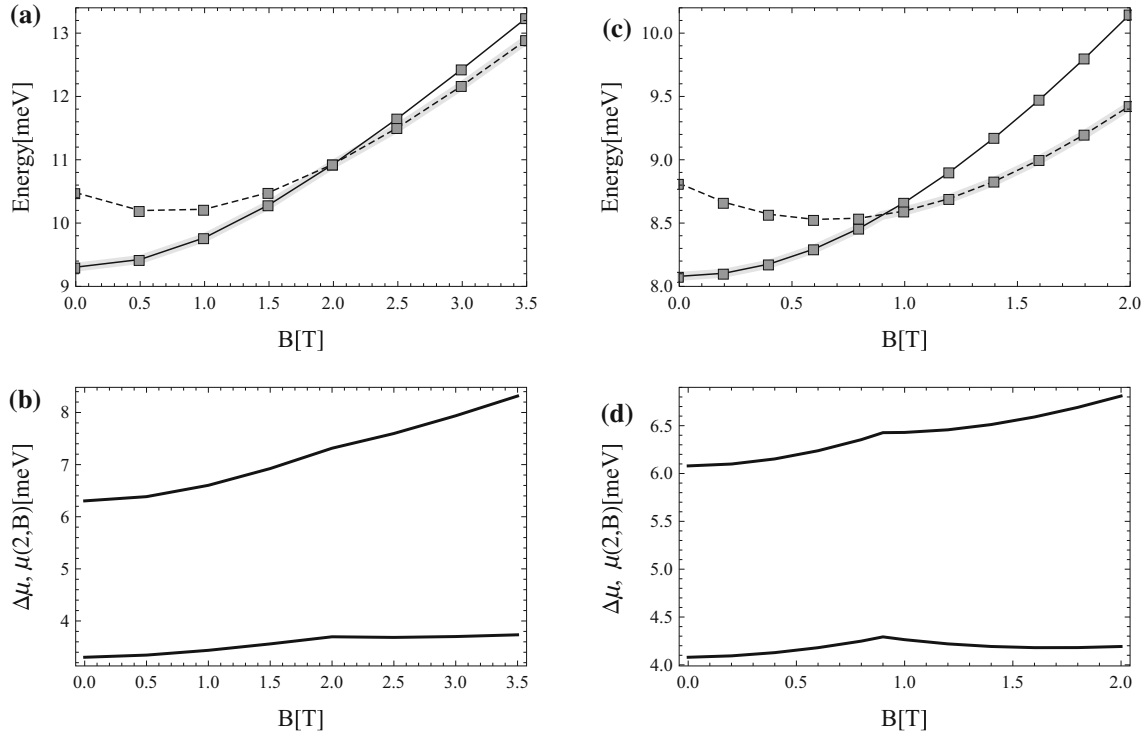


Fig. 2 Dependence on the magnetic field of: **a** singlet state (black, solid line), triplet state (black, dashed line), ground state (gray, solid line) of a 3D QD and **b** chemical potential $\mu(2, B)$ (upper line) and addition energy $\Delta\mu = \mu(2, B) - \mu(1, B)$ (lower line) of a 3D QD. The same is given in **(c)** and **(d)** for a 2D QD. Confinement frequency $\hbar\omega_0 = 2 \text{ meV}$

parameters $\Omega_0 = \hbar\omega_0/\hbar\omega_h$ and $\gamma = B/B_0$ are calculated with $\hbar\omega_h = E_h = 27.211 \text{ eV}$ and $B_0 = 2.35 \times 10^5 \text{ T}$. One can note that, as the result of different slopes of energy curves belonging to singlet and triplet levels, the cusps are observed in the B -dependence of the ground state energy, at the magnetic fields corresponding to the ST transitions. As a consequence, similarly behave also the chemical potential and the addition energy $\Delta\mu$.

As can be seen in Fig. 2, presence of the third dimension leads to increasing of magnetic fields inducing the ST transitions. The additional effect is *damping* of the cusps occurring in the B -field dependence of the observables being functions of the ground state energy. We can note that effects related to the third dimension are important from a point of view of experimental study of magnetic properties of a quasi two-dimensional QD where the vertical diameter of the dot becomes significant [21, 22]. One of the most important statements given

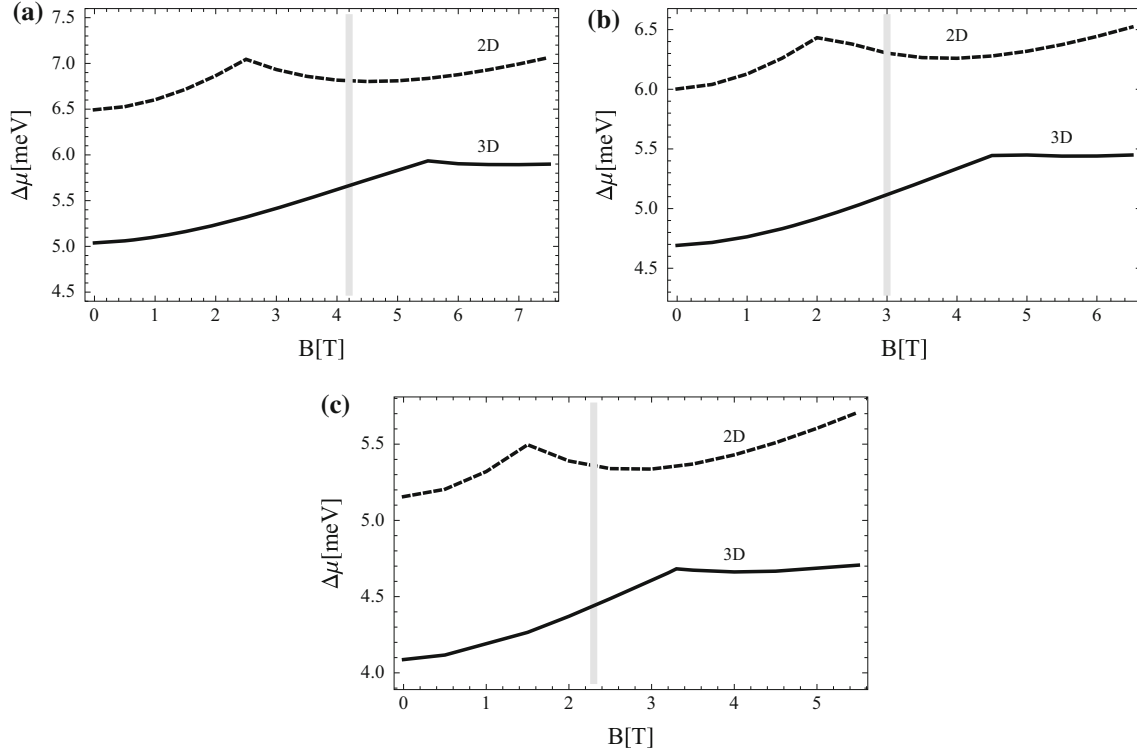


Fig. 3 Magnetic dependence of the addition energy $\Delta\mu$ in two-electron 2D (dashed lines) and 3D (solid lines) QDs with confinement: **a** $\hbar\omega_0 = 4.2$ meV, **b** $\hbar\omega_0 = 3.7$ meV and **c** $\hbar\omega_0 = 2.9$ meV. The solid gray lines display the experimental positions of the first ST transitions points, respectively: 4.2, 3 and 2.3 T [21]

in the literature on this problem is that the experimental positions of the ST transition points are systematically higher than reproduced by the 2D calculations [22]. In Fig. 3 are presented the addition energies as functions of the magnetic field, calculated within the 2D and 3D models. Confinement energies $\hbar\omega_0$ are taken into account with 'experimental' values [21]. We can see that the 3D isotropic model gives values of the magnetic fields for the first ST transitions which exceed experimental values. Although, we not reproduced exactly the experimental positions of the first ST transitions (approximately, they have the same deviations from the experimental values as in the 2D model, but of opposite signs), results obtained in this work are important for understanding the basic source of discrepancy between the theoretical 2D calculations and experimental data. Evidently, this inconsistency is caused by the influence of the third dimension. Moreover, experimental curves (not plotted in Fig. 3) are located in the region limited by curves of the 2D and 3D models (see Fig. 1 in [22]). This means that there exists such a deformation of a 3D QD that may give good approximation to realistic system. The anisotropic 3D model has been recently considered by introducing finite parabolic confinement in the z -direction, that allowed to reproduce some experimental data. The confinement in the third dimension $\hbar\omega_z = 8$ meV has been estimated to provide the best fit for the positions of kinks in the additional energy [22].

5 Summary

We have carried out theoretical analysis of the dynamics of two interacting electrons placed in an external magnetic field, in three spatial dimensions. Approximate solutions have been obtained based on the power-series expansion method and appropriate boundary conditions. Energies of the HA have been obtained with higher accuracy than previous most accurate results, obtained using the spherical harmonic expansion and the Landau orbital expansion [27]. The solutions have been obtained also for a wider range of B . This allowed us to study continuous transition to the 1D model, corresponding to the limit of extremely strong magnetic field.

Under some assumptions the HA may be regarded to as a two-electron QD. We have studied ground-state magnetic properties of the semiconductor QD's, using parameters typical for GaAs. The 3D and 2D models have been studied as cases, described by anisotropy parameters $a \leq 1$ (spherical or a prolate QD) and $a = \infty$

(2D QD). The method, presented in this paper, is applicable also to the case $a > 1$ (an *oblate* QD). In this case, the expansion in powers of $r \sin \vartheta$ should be replaced by an expansion in powers of $r \cos \vartheta$. Both methods are complementary. The model of an elliptically deformed QD (of an *oblate* type) adjusted for description of vertically extended QDs along with the problem of a continuous transition to the 2D limit shall be investigated elsewhere.

Open Access This article is distributed under the terms of the Creative Commons Attribution 4.0 International License (<http://creativecommons.org/licenses/by/4.0/>), which permits unrestricted use, distribution, and reproduction in any medium, provided you give appropriate credit to the original author(s) and the source, provide a link to the Creative Commons license, and indicate if changes were made.

References

1. Jaskólski, W.: Confined many-electron systems. *Phys. Rep.* **271**, 1 (1996)
2. Birmana, J.L., Nazmitdinov, R.G., Yukalov, V.I.: Effects of symmetry breaking in finite quantum systems. *Phys. Rep.* **526**, 1 (2013)
3. Sako, T., Diercksen, G.H.F.: Confined quantum systems: spectral properties of two-electron quantum dots. *J. Phys. Condens. Matter* **15**, 5487 (2003)
4. Debeloa, N.G., Dejenea, F.B., Malnevb, V.N., Senbetab, T., Mesfinb, B., Roro, K.: Effect of retrapping on thermoluminescence peak intensities of small amorphous silicon quantum dots. *Acta Phys. Pol. A* **129**, 362 (2016)
5. Kościk, P., Saha, J.K.: Ground-state entanglement properties of helium atom in a finite spherical cavity. *Few Body Syst.* **56**, 645 (2015)
6. Kestner, N.R., Sinanoğlu, O.: Study of electron correlation in helium-like systems using an exactly soluble model. *Phys. Rev.* **128**, 2687 (1962)
7. Lopez, X., Ugalde, J.M., Echevarría, L., Ludeña, E.V.: Exact non-Born-Oppenheimer wave functions for three-particle Hookean systems with arbitrary masses. *Phys. Rev. A* **74**, 042504 (2006)
8. Karwowski, J.: A separable model of N interacting particles. *Int. J. Quantum Chem.* **108**, 2253 (2008)
9. Taut, M.: Two electrons in an external oscillator potential: particular analytic solutions of a Coulomb correlation problem. *Phys. Rev. A* **48**, 3561 (1993)
10. Taut, M.: Two electrons in a homogeneous magnetic field: particular analytical solutions. *J. Phys. A Math. Gen.* **27**, 1045 (1994)
11. Maksym, P.A., Chakraborty, T.: Quantum dots in a magnetic field: role of electron–electron interactions. *Phys. Rev. Lett.* **65**, 108 (1990)
12. Merkt, U., Huser, J., Wagner, M.: Energy spectra of two electrons in a harmonic quantum dot. *Phys. Rev. B* **43**, 7320 (1991)
13. Wagner, M., Merkt, U., Chaplik, A.V.: Spin-singletspin-triplet oscillations in quantum dots. *Phys. Rev. B* **45**, 1951 (1992)
14. Ashoori, R.C., Stormer, H.L., Weiner, J.S., Pfeiffer, L.N., Baldwin, K.W., West, K.W.: N-electron ground state energies of a quantum dot in magnetic field. *Phys. Rev. Lett.* **71**, 613 (1993)
15. Kais, S., Herschbach, D.R., Handy, N.C., Murray, C.W., Laming, G.J.: Density functionals and dimensional renormalization for an exactly solvable model. *J. Chem. Phys.* **99**, 417 (1993)
16. Madhav, A.V., Chakraborty, T.: Electronic properties of anisotropic quantum dots in a magnetic field. *Phys. Rev. B* **49**, 8163 (1994)
17. Fujito, M., Natori, A., Yasunaga, H.: Many-electron ground states in anisotropic parabolic quantum dots. *Phys. Rev. B* **53**, 9952 (1996)
18. Dineykh, M., Nazmitdinov, R.G.: Two-electron quantum dot in a magnetic field: analytical results. *Phys. Rev. B* **55**, 13707 (1997)
19. Nazmitdinov, R.G., Simonović, N.S., Rost, J.M.: Semiclassical analysis of a two-electron quantum dot in a magnetic field: dimensional phenomena. *Phys. Rev. B* **65**, 155307 (2002)
20. Simonović, N.S., Nazmitdinov, R.G.: Hidden symmetries of two-electron quantum dots in a magnetic field. *Phys. Rev. B* **67**, 041305(R) (2003)
21. Nishi, Y., Tokura, Y., Gupta, J., Austing, G., Tarucha, S.: Ground-state transitions beyond the singlet-triplet transition for a two-electron quantum dot. *Phys. Rev. B* **75**, 121301(R) (2007)
22. Nazmitdinov, R.G., Simonović, R.S.: Finite-thickness effects in ground-state transitions of two-electron quantum dots. *Phys. Rev. B* **76**, 193306 (2007)
23. Nazmitdinov, R.G., Simonović, R.S., Plastino, A.R., Chizhov, A.V.: Shape transitions in excited states of two-electron quantum dots in a magnetic field. *J. Phys. B At. Mol. Opt. Phys.* **45**, 205503 (2012)
24. Drouvelis, P.S., Schmelcher, P., Diakonov, F.K.: Global view on the electronic properties of two-electron anisotropic quantum dots. *Phys. Rev. B* **69**, 035333 (2004)
25. Szafran, B., Peeters, F.M., Bednarek, S., Adamowski, J.: Anisotropic quantum dots: correspondence between quantum and classical Wigner molecules, parity symmetry, and broken-symmetry states. *Phys. Rev. B* **69**, 125344 (2004)
26. Zhu, W., Trickey, S.B.: Analytical solutions for two electrons in an oscillator potential and a magnetic field. *Phys. Rev. A* **72**, 022501 (2005)
27. Zhu, W., Trickey, S.B.: Exact density functionals for two-electron systems in an external magnetic field. *J. Chem. Phys.* **125**, 094317 (2006)

-
28. Movilla, J.L., Planelles, J., Jaskólski, W.: From independent particles to Wigner localization in quantum dots: the effect of the dielectric environment. *Phys. Rev. B* **73**, 035305 (2006)
 29. Kościk, P., Okopińska, A.: Two-electron entanglement in elliptically deformed quantum dots. *Phys. Lett. A* **374**, 3841 (2010)
 30. Holovatski, V., Bernik, I., Voitsekhivska, O.: Oscillator strengths of quantum transitions in spherical quantum dot GaAs/Al_xGa_{1-x}As/ GaAs/Al_xGa_{1-x}As with on-center donor impurity. *Acta Phys. Pol. A* **125**, 93 (2014)
 31. Kravchenko, YuP, Liberman, M.A., Johansson, B.: Exact solution for a hydrogen atom in a magnetic field of arbitrary strength. *Phys. Rev. A* **54**, 287 (1996)
 32. Rutkowski, A., Poszwa, A.: Hydrogen atom in a strong magnetic field. *Phys. Rev. A* **67**, 013412 (2003)
 33. Poszwa, A., Rutkowski, A.: Static dipole magnetic susceptibilities of relativistic hydrogenlike atoms: a semianalytical approach. *Phys. Rev. A* **75**, 033402 (2007)
 34. Poszwa, A.: Relativistic two-dimensional H-like model atoms in an external magnetic field. *Phys. Scr.* **84**, 055002 (2011)
 35. Fock, V.: Bemerkung zur Quantelung des harmonischen Oszillators im Magnetfeld. *Z. Phys.* **47**, 446 (1928)
 36. Darwin, C.G.: The diamagnetism of the free electron. *Proc. Camb. Philos. Soc.* **27**, 86 (1930)
 37. Abramowitz, M., Stegun, I.A.: *Handbook of Mathematical Functions*. Dover, New York (1968)